MOKSLAS – LIETUVOS ATEITIS
SCIENCE – FUTURE OF LITHUANIA
ISSN 2029-2341 / eISSN 2029-2252
http://www.mla.vgtu.lt

STATYBA, TRANSPORTAS, AVIACINĖS TECHNOLOGIJOS
CIVIL AND TRANSPORT ENGINEERING, AVIATION TECHNOLOGIES

2014 6(5): 531–537

Transportas
Transport Engineering

http://dx.doi.org/10.3846/mla.2014.696

A MATHEMATICAL MODEL AND SIMULATION RESULTS OF THE DYNAMIC SYSTEM *RAILWAY VEHICLE WHEEL–TRACK* WITH A WHEEL FLAT

Rasa ŽYGIENĖ[1], Marijonas BOGDEVIČIUS[2], Laima DABULEVIČIENĖ[3]
Vilnius Gediminas Technical University
E-mails: [1]rasazz@gmail.com; [2]marijonas.bogdevicius@vgtu.lt; [3]laima.dabuleviciene@vgtu.lt

Abstract. A mathematical model of the system *Railway Vehicle Wheel–Track* with a wheel flat of a wheelset has been made. The system *Railway Vehicle Wheel–Track* has been examined on the vertical plane. The mathematical model of the system *Railway Vehicle Wheel–Track* has employed linear, nonlinear, elastic and damping discrete elements. Rail dynamics haves been described using the finite element method. The unevenness of the rail and the wheel of the wheelset have been evaluated considering the contact between the rail and the wheel flat of the wheelset. The analysis of dynamic processes taking place in a railway vehicle wheel with the wheel flat moving at speed V = 60 km/h has been accomplished. The results of mathematical modelling of the above introduced dynamic system have been presented along with graphically displayed research findings of the conducted research.

Keywords: wheel-rail contact, dynamics, acceleration, penetration, numerical method.

Introduction

Rail traffic safety, power output, fuel efficiency, track usage, etc. depend on the wheel-rail interaction of a railway vehicle. The distribution of forces resulting from wheel-rail interaction influences the wheel of the railway vehicle and track dynamics. Interaction forces affecting the wheel of the railway vehicle and the rail occur in the contact of the wheel having a defect and the rail. The extent of contact force directly depends upon the velocity of the railway vehicle, wheel-rail geometric parameters as well as physical and mechanical characteristics of the system *Railway Vehicle Wheel–Track*. Therefore, the majority of defects are detected on the rail head and tread surface.

One of the most common numerical methods are the finite element method. When analysing the wheel-rail interaction of the railway vehicle, the theories evaluating forces resulting from the wheel-rail interaction of the railway vehicle are used, *Hertz, Kalker, "Johnson, Kendall, Roberts" (JKR), Bradley*, etc.

The *Hertz theory* of elastic bodies is the most popular one stating that if two bodies are compressed, the contact area is elliptical in shape and is formed in the centre of maximum pressure. Having integrated pressure distribution in the contact area, it is possible to determine the maximum load.

The mathematical model of railway vehicle wheels and a track (Ferrara *et al.* 2012) has been designed to explore the dynamics of the railway vehicle.

Research on the interaction between a wheel with a flat and the rail has been carried out (Zhu *et al.* 2007) when a wheel flat is 100 mm and the railway vehicle is moving at different speeds. The values of the maximum strength emerging in wheel-rail interaction are compared to the *Hertz theory*. The article states that an adaptive model for calculating the length and depth of contact with possible wheel profile asymmetry that allows the exploration of forces arising between the wheel and the rail has been developed. The effect of forces on vertical vibrations in adjacent wheels has been determined.

The articles (Wu, Thompson 2001) have examined the interaction between a railway track and a moving train and evaluated the irregularities of the track, damage to the wheelset, the axial load of the rail, etc. A mathematical model of the railway vehicle wheelset having the wheel flat and rail interaction have been designed (Uzzal 2012), which allows determining forces arising from the interaction and prediction of their noise. It has been found that if the railway vehicle is moving faster than 30 km/h, contact is lost when wheel flats are 2 mm deep and 86 mm in length. It is also argued that an increase in speed and wheel load may also increase noise level.

The articles by (Nielsen, Oscarsson 2004) examine the interaction of the railway train wheelset with the wheel flat and the rail on the vertical plane. Studies were performed when the length of the wheel flat was 100 mm and depth – 0.9 mm. Test results (Wasiwitono *et al.* 2007) on forces showed that the interaction between the wheel flat and the rail was dependant on different axial forces acting into the rail and the speed of the train.

The analysis of scientific papers has revealed there is no single method for determining the dynamics of the interaction between the railway vehicle wheelset with wheel flat and the rail. The article analyses the dynamic processes of the system *Railway Vehicle Wheel–Track* (Fig. 1) moving at speed V = 60 km/h.

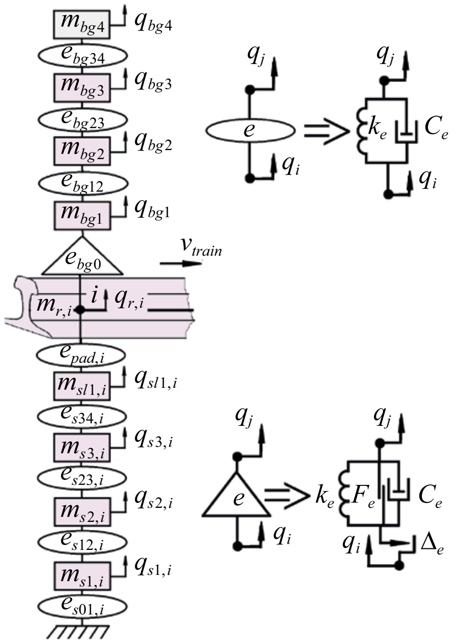

Fig. 1. Dynamic model of the system *Railway Vehicle Wheel–Track*: (a) scheme; (b) nonlinear elastic–damping discrete element, (c) linear elastic–damping discrete element

Mathematical model of
Railway Vehicle Wheel–Track

The dynamics of the rail has been considered using the finite element method. The finite element is applied in the two node beam element with rail unevenness (see Figure 2).

Displacement vector and the initial displacement of the beam finite element are equal to:

$$w = \left[N_w(\xi)\right]\{q_e\},\; w_0 = \left[N_w(\xi)\right]\{w_{0e}\}, \qquad (1)$$

where $\{w_{0e}\}$ – displacement vector; w – displacement vectors along axes X and Z; $\{q_e\}$ – displacement vector;

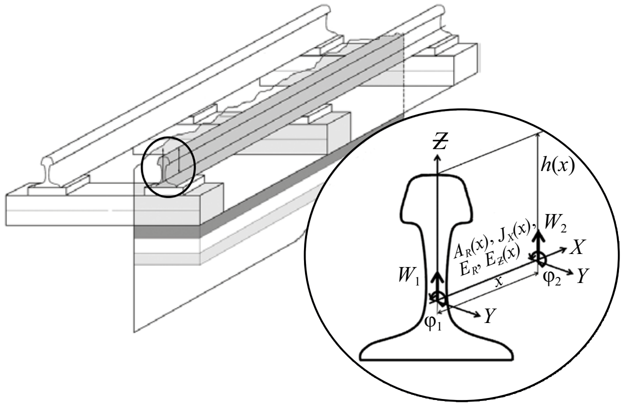

Fig. 2. Parameters assessing rail unevenness

$\left[N\left(\xi = x/L_e\right)\right]$ – the matrix of shape functions where $\xi = x/L_e$ – a local coordinate; L_e – the length of the finite element.

The potential energy of beam finite element E_p consists of the potential energy of bending $E_{p,b}$, tension force $E_{p,T}$ and elastic foundation $E_{p,F}$,

$$E_p = E_{p,b} + E_{p,T} + E_{p,F}\,. \qquad (2)$$

$$E_{p,b} = \frac{1}{2}\int_0^{L_e} EJ_Y(x)\left(\frac{\partial^2 w}{\partial x^2} - \frac{\partial^2 w_0}{\partial x^2}\right)^2 dx,$$
$$E_{p,T} = \frac{1}{2}\int_0^{L_e} F_a\left(\frac{\partial w}{\partial x} - \frac{\partial w_0}{\partial x}\right)^2 dx, \qquad (3)$$
$$E_{p,F} = \frac{1}{2}\int_0^{L} k_S(x)\left(w(x) - w_0(x)\right)^2 dx,$$

where E – the modulus of rail elasticity; $J_Y(x)$ – the axial moment of inertia; F_a – axial force; $k_S(x)$ – the coefficient of the stiffness of elastic foundation.

The system of equations for sleepers, ballast and sub ballast blocks are established from *Lagrange* equation of the second order:

$$\left[M_{i,j}\right]\left\{\ddot{q}_{i,j}\right\} + \left[C_{i,j}\right]\left\{\dot{q}_{i,j}\right\} + \left[K_{i,j}\right]\left\{q_{i,j}\right\} = \left\{F_{i,j}\right\}, \qquad (4)$$

where $\left[M_{i,j}\right]$, $\left[C_{i,j}\right]$, $\left[K_{i,j}\right]$ – mass, damping and stiffness matrices of the ballast and sub– ballast block and a part of the rail; $\left\{q_{i,j}\right\}, (k+1), \left\{\ddot{q}_{i,j}\right\}$ – displacement vectors, the velocity and acceleration of ballast, sleeper and rail,

$$\left\{q_{i,j}\right\}^T = \left[\left\{q_{bi}\right\}^T \; \left\{q_{bj}\right\}^T \; \left\{q_{Rij}\right\}^T\right], \qquad (5)$$

$\{q_{bi}\}, \{q_{bj}\}, \{q_{Rij}\}$ – displacement vectors of the ballast and sub ballast block and a part of the rail:

$$\left\{q_{bi}\right\}^T = \left[q_{sl,i} \;\; q_{s1,i} \;\; q_{s2,i} \;\; q_{s3,i}\right],$$

$$\left\{q_{bj}\right\}^T = \left[q_{sl,j} \;\; q_{s1,j} \;\; q_{s2,j} \;\; q_{s3,j}\right],\; \left\{q_{Rij}\right\}^T = \left[w_i, w_j\right].$$

Irregularities of the rail are described as function $\Delta Z_R(x)$. The profile of the railway wheel is defined as a function of radius $R_W(\theta)$ and depends on polar angle θ.

The profile of the railway wheel is defined as a function of a variable radius depending on the polar angle. Radius $R_W(\theta)$ of the wheel profile is described by *Fourier series*:

$$R_W(\theta)=\sum_{k=1}^{NH} a_{ck}\cos(k\theta)+a_{sk}\sin(k\theta), \tag{6}$$

where a_{ck}, a_{sk} – *Fourier* coefficients; *NH* – the number of harmonics.

While under operation, the profile of the rail-wheel changes and affects rail-wheel – rail interaction. Rail wheel flats are most commonly caused by the uneven surface, temperature differences, etc. Axle wheel flats occur on the tread surface. Wheel damage is usually determined visually or by template support, depending on the qualifications of the staff. Other diagnostic methods are also used for having control on the rolling surface. For example, by applying *Lenz* and vibrant force sensors, the critical values of the wheel surface are measured by comparison.

When determining rail – wheel-rail intersection points, it is necessary to know the coordinates of the rail-wheel and rails *X* and *Z*.

Penetration rate at point k with local coordinate ξ_{ck} of the contact is:

$$\delta_k=[N_w(\xi_k)]\{q_e\}+\Delta Z_R\cos(\varphi_k)-\left(q_{bg1}-\left(R_{W0}-R_k(\Psi_k)\right)\sin(\Psi_k)\right), \tag{7}$$

where R_{W0} – a nominal diameter of the rail–wheel; $R_k(\Psi_k)$ – the radius of the rail–wheel profile; q_{bg1} – the vertical displacement of the rail–wheel; $\{q_e\}$ – the displacement vector of the rail finite element; Ψ_k – angle (Fig. 3).

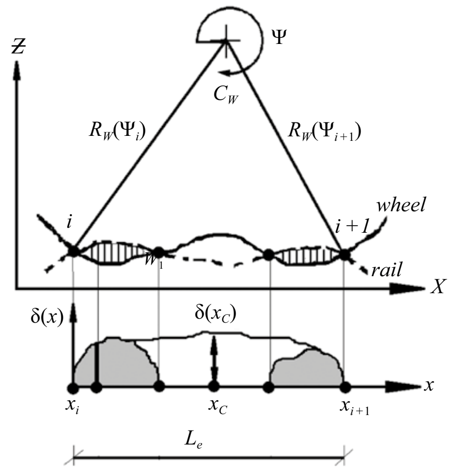

Fig. 3. Geometric parameters of the contact area of the wagon wheel and the rail

Force k appearing at the contact point is determined by the *Hertz theory* and formula:

$$F_{contact}(x)=k_{bg0}(x)\delta(x)^n D\left(\dot{\delta}(x)\right)H\left(\delta(x)\right), \tag{8}$$

where

$$k_{bg0}(x)=\frac{4}{3}E_{ekv}\sqrt{R(x)},\quad \frac{1}{E_{ekv}}=\frac{1-\nu_R^2}{E_R}+\frac{1-\nu_W^2}{E_W},$$

$$\frac{1}{R(x)}=\frac{1}{R_R(x)}+\frac{1}{R_W(x)},$$

$$D_{ck}(\dot{\delta}_k)=1+\frac{3}{4}\left(1-e_k^2\right)\frac{\dot{\delta}_k}{\dot{\delta}_{\max}},$$

$$R_R(x_k)=\left[1+\left(\frac{d\Delta Z_R(x_k)}{dx}\right)^2\right]^{\frac{3}{2}}\left(\frac{d^2\Delta Z_R(x_k)}{dx^2}\right)^{-1},$$

and where k_{bg0} – contact stiffness; e_k – speed restitution coefficient; E_R, E_W – the modulus of elasticity of the rail and the wheel; ν_R, ν_W – Poisson's coefficients.

In the contact area, load distribution in interval $x\in[x_1\dots x_{NP}]$ is equal to:

$$q(x)=\frac{dF_{contact}(x)}{dx}=\frac{dF_{contact}(x)}{dk}\frac{dk(x)}{dx}+\frac{dF_{contact}(x)}{dR}\frac{dR(x)}{dx}+\frac{dF_{contact}(x)}{d\delta}\frac{d\delta(x)}{dx}. \tag{9}$$

The load vector of the finite element of the *e–th* rail in contact length is equal to:

$$\{F_e\}=\sum_{i=1}^{ne}\int_{\xi_i}^{\xi_{i+1}}\left[N_w(\xi)\right]^T q(\xi)L_e d\xi, \tag{10}$$

where *ne* – the number of contact intervals in the rail finite element when penetration, in all contact interval $\xi\in[\xi_i,\xi_{i+1}]$, is positive, $\delta\ge 0$.

In the contact interval, vertical force acts to the first body of the wheel and is equal to:

$$F_{BW}=\sum_e\sum_{i=1}^{ne}\int_{\xi_i}^{\xi_{i+1}} q_e(\xi)L_e d\xi. \tag{11}$$

The general equation system (Fig. 2) of all movement systems is equal to:

$$[M]\{\ddot{q}\}+[C]\{\dot{q}\}+[K]\{q\}+\{F_{NL}(q,\dot{q})\}=\{F(t)\}, \tag{12}$$

where $\{q\}^T=\left[\{q_R\}^T,\{q_B\}^T,\{q_{bg}\}^T\right]$ – displacement vector; $\{q_R\}$ – rail displacement vector; $\{q_S\}$ – ballast displacement vector; $\{q_{bg}\}$ – rail vehicle displacement vector.

Numerical results of dynamic processes in the system *Railway Vehicle Wheel–Track*

The system *Railway Vehicle Wheel–Track* uses data on the four–axle freight wagon 12–9780. It is assumed that the wagon moves at a speed of 60 km/h chosen randomly at our discretion. The flat of the wagon wheel is L = 100 mm. A static load on the rail is 100 kN. Rail R65 of 16.2 m in length has been analysed. The distance between sleepers is 0.5435 m and is divided into 10 beam finite elements. Integration time step is $\Delta t = 5 \cdot 10^{-6}$ s. The profile of the railway wagon with the wheel flat is described using the two hundred harmonic $NH = 201$. The total number of unknowns is 730. Calculations have been performed applying our developed program and using Fortran software. The parameters of the developed system are presented in Table 1.

The wheel loses contact with the railway track due to the rail, sleepers, the high stiffness of the rail bed and low damping, dynamic properties, a high speed of the wagon and a significant wheel flat. Changes in wheel radius over time are shown in Figure 4.

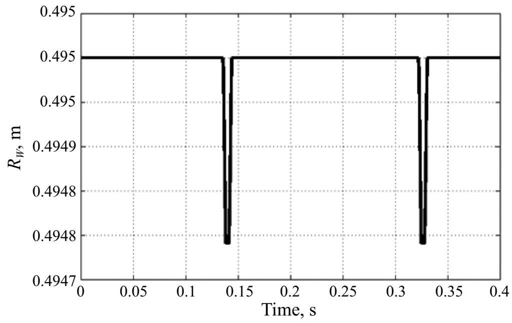

Fig. 4. Changes in radius R_w of the railway wheelset with the flat (L = 100 m) over time

Table 1. Parameters of the system *Railway Vehicle Wheel–Track*

Railway track			
Force of axial loading	$F_x = 0$ kN	ballast damping coefficient:	$C_{s11,\,i,j} = 10$ kNs/m
The second moment of the area of the rail about Y	$J_R = 3.54 \cdot 10^{-5}$ m^4	$C_{s22,\,i,j} = 13$ kNs/m	$C_{s33,\,i,j} = 15$ kNs/m
Cross-sectional area of the rail	$A_R = 82.65 \cdot 10^{-4}$ m^2	$C_{s01} = 90$ kNs/m	$C_{s12} = 70$ kNs/m
Poisson's coefficient of the rail	$\nu_R = 0.30$	$C_{s23} = 60$ kNs/m	$C_{s34} = 50$ kNs/m
Elastic modulus of the rail	$E_R = 206$ GPa	ballast stiffness coefficient:	$k_{s11,\,i,j} = 15$ MN/m
Rail density	$\rho_R = 7850$ kg/m^3	$k_{s22,\,i,j} = 16$ MN/m	$k_{s33,\,i,j} = 17$ MN/m
Rail mass per meter	$m_R = 65$ kg/m	$k_{s01} = 180$ MN/m	$k_{s12} = 170$ MN/m
Pad damping coefficient	$C_{pad} = 45$ kNs/m	$k_{s23} = 160$ MN/m	$k_{s34} = 150$ MN/m
Pad stiffness	$k_{pad} = 140$ MN/m	ballast mass:	$m_{s1} = 500$ kg
Sleeper spacing	$L_p = 0.5435$ m	$m_{s2} = 300$ kg	$m_{s3} = 200$ kg
Sleeper mass	$m_{sl} = 265$ kg	friction coefficient	$\mu\left(\varepsilon_{e,i}\right) = 0.3$
Railway vehicle			
1/8 car body mass	$m_{bg4} = 8743$ kg	car body damping coefficient	$C_{bg4} = 10$ kNs/m
1/4 bogie mass	$m_{bg3} = 700$ kg	frame damping coefficient	$C_{bg3} = 100$ kNs/m
1/2 wheelset mass	$m_{bg2} = 640$ kg	wheelset damping coefficient	$C_{bg2} = 50$ kNs/m
Mass in contact	$m_{bg1} = 110$ kg	damping coefficient of mass in contact	$C_{bg1} = 44.2$ kNs/m
Car body stiffness	$k_{bg34} = 2.55$ MN/m	wheel Radius	$R_W = 0{,}495$ m
Frame stiffness	$k_{bg23} = 6.5$ MN/m	elastic modulus of wheel	$E_W = 210$ GPa
Wheelset stiffness	$k_{bg12} = 56$ MN/m	restitution coefficient	$\dot{\delta}_{\max} = 10$ m/s
Maximal penetration velocity	$\dot{\delta}_{\max} = 10$ m/s	Poisson's coefficient of wheel	$e = 0.65$
Exponent	$n = 3/2$		

Rail displacements and accelerations are shown in Figures 5 and 6.

The shifts of rail displacements in time when the velocity of the train is 60 km/h at different nodes of the finite element like 31-th node (4-th sleeper), 41-th node (5-th sleeper), 51-th node (6-th sleeper) (d) 61-th node (7-th sleeper); (e) 71-th node (8-th sleeper) are shown in Figure 5.

The shifts of rail accelerations in time, when the velocity of the train is 60 km/h at different nodes of the finite element, including (a) 31-th node (4-th sleeper); (b) 41-th node (5-th sleeper); (c) 51-th node (6-th sleeper); (d) 61-th node (7-th sleeper); (e) 71-th node (8-th sleeper), are shown in Figure 6.

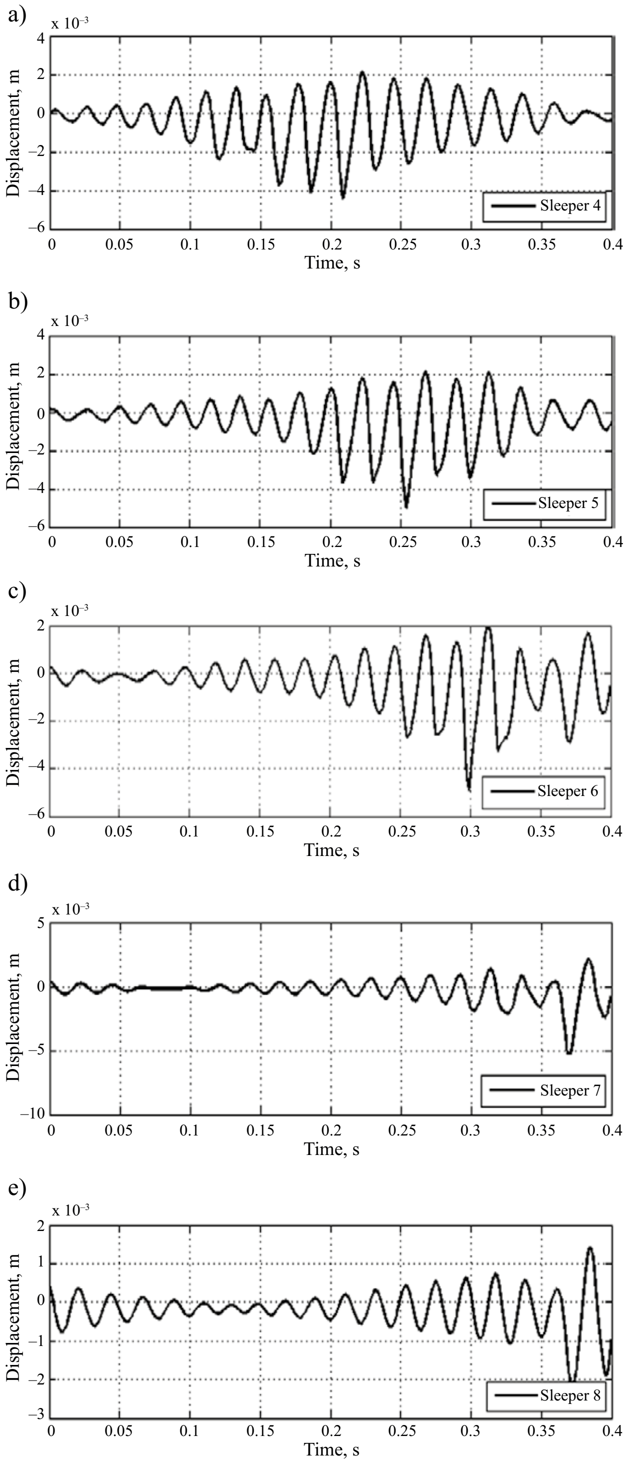

Fig. 5. Displacements of the rail at different nodes of the finite element: (a) 31-th node; (b) 41-th node; (c) 51-th node; (d) 61-th node; (e) 71-th node

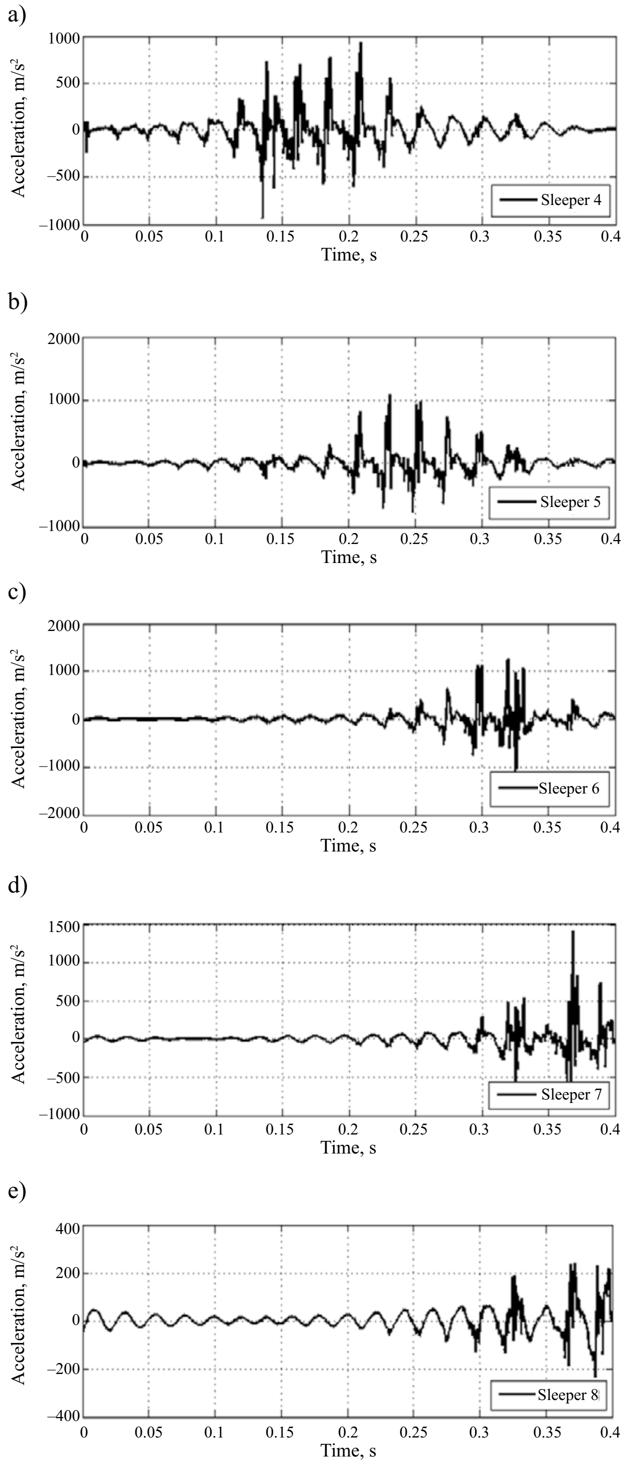

Fig. 6. Accelerations of the rail when the velocity of the train is 60 km/h at different nodes of the finite element: (a) 31-th node; (b) 41-th node; (c) 51-th node; (d) 61-th node; (e) 71-th node

Penetration describes the contact between the wagon wheel and the rail. When the value of penetration is positive ($\delta \geq 0$), the wheel is in contact with the rail; however, when penetration is negative ($\delta < 0$) the wheel is not in contact with the rail. Changes in penetration δ in the centre of the contact of the moving wagon with the flat and the rail over time are shown in Figure 7.

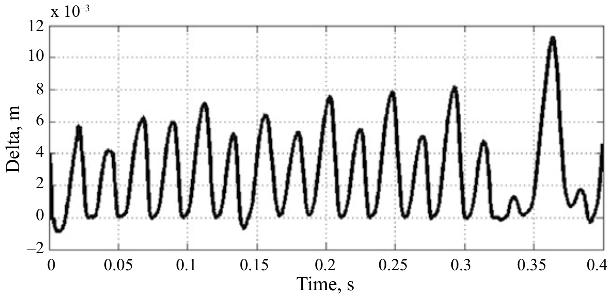

Fig. 7. Changes in penetration $\delta(t)$ over time

First and second order time derivatives of penetration are shown in Figures 8 and 9.

The dependency of load distribution on the railway vehicle, when velocity $V = 60$ km/h and the length of wheel flat $L = 100$ mm, is shown in Figure 10.

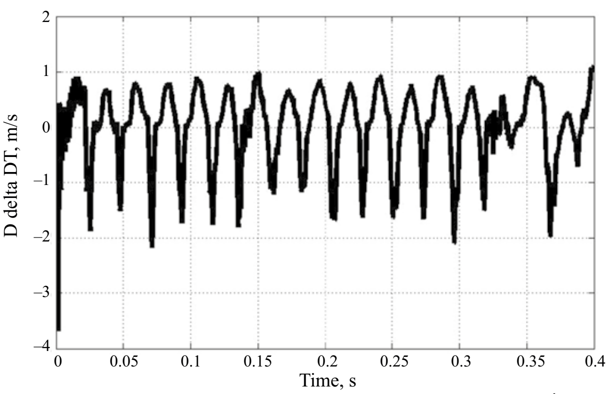

Fig. 8. Changes in the time derivative of penetration $\dot{\delta}(t)$ over time

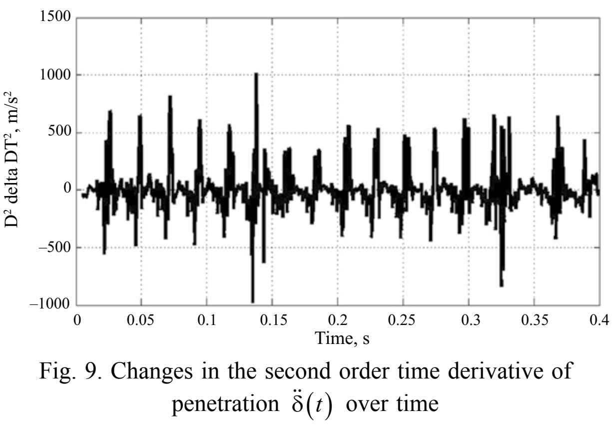

Fig. 9. Changes in the second order time derivative of penetration $\ddot{\delta}(t)$ over time

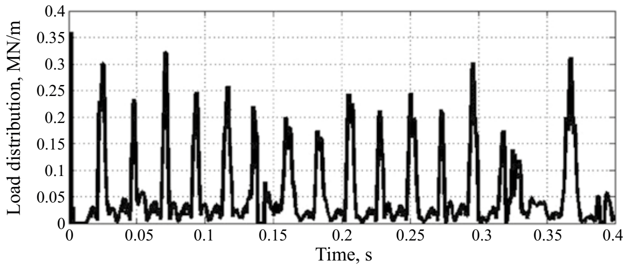

Fig. 10. The dependency of load distribution (9) on the railway vehicle under velocity V = 60 km/h

Changes in of the railway vehicle wheelset with accelerations of the flat over time are shown in Figure 11.

Along with an increase in the speed of the railway vehicle and the vertical load of the wheel on the rail, maximum vertical acceleration increases in the railway vehicle wheelset.

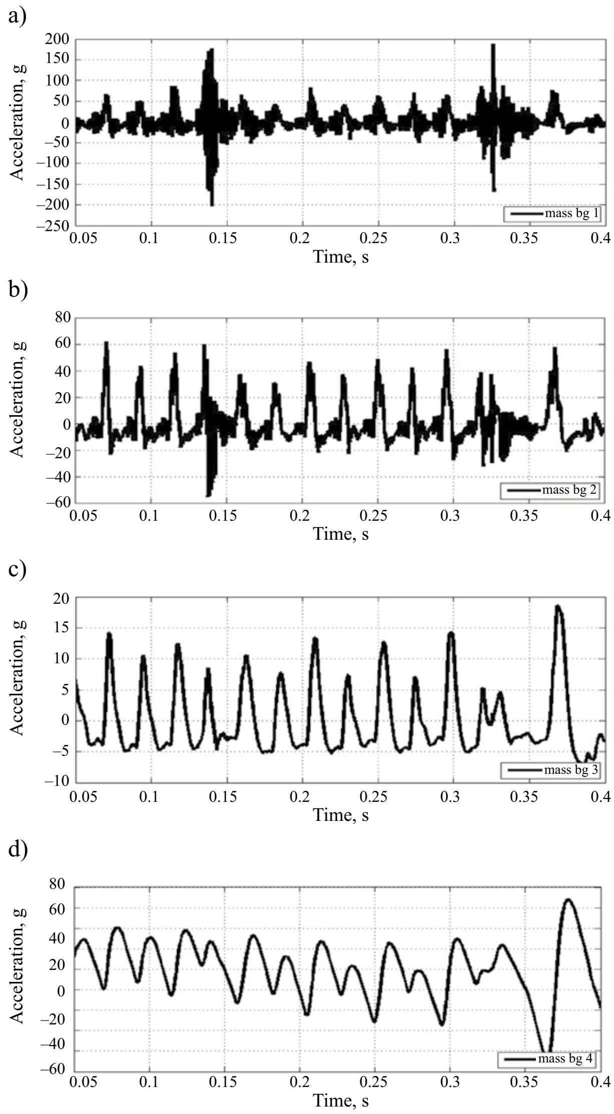

Fig. 11. Changes in the railway vehicle wheelset with vertical accelerations of the flat (L = 100 mm) over time:
(a) car body; (b) frame; (c) wheelset; (d) contact mass

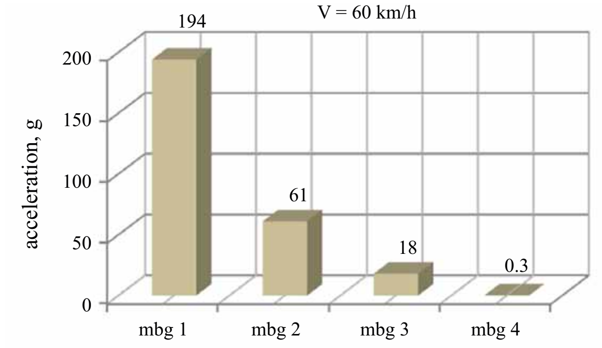

Fig. 12. A comparison of vertical accelerations of the mass of the wagon

A comparison of the vertical acceleration of the mass of the wagon with the wheel flat, under the wagon velocity of 60 km/h, is shown in Figure 12.

A comparison of the vertical accelerations of the masses (Fig.12) of the wagon with the wheel flat provides that acceleration decreases due to different physical and mechanical parameters of masses.

Conclusions

1. The developed mathematical model of the system *Railway Vehicle Wheel–Track* enables to examine the interaction between the wheel flat and the rail and to assess the soil of the rail bed, sleepers and intermediary physical and mechanical properties, wheel geometry, the dynamic characteristics of the wagon at different running speeds and the sizes of wheel flats. Research on the dynamic processes of the system *Railway Vehicle Wheel–Track* with wheel flat $L = 100$ mm under speed $V = 60$ km/h shows that the static load of the wheel is equal to 0.1 MN.
3. When the speed of the wagon is 60 km/h and the wheelset with the wheel flat is in contact with the rail, the wheelset wheel loses its contact with the rail once after the impact.
4. When the railway vehicle wheelset with the flat is moving at a speed of 60 km/h, during 0.4 s, two impacts occur at wheel – rail contact. The first impact takes place in 0.14 s and the second one occurs in 0.32. Penetration is negative at 0.14 s and 0.32 s, and the wheel of the wheelset loses contact with the rail for a short time. The value of the vertical acceleration of mass m_{bg1} is at maximum in 0.14 s and 0.32 s.
5. When the length of the wheelset with the wheel flat is 100 mm and the speed of the wagon is 60 km/h, the vertical acceleration of the wheelset wheel is equal to 61 g.

Acknowledgements

This work has been supported by the European Social Fund within the project *Development and Application of Innovative Research Methods and Solutions for Traffic Structures, Vehicles and Their Flows*, project code VP1–3.1–ŠMM–08–K–01–020.

References

Ferrara, R.; Leonardi, G.; Jourdan, F. 2012. Numerical modelling of train induced vibrations, *Procedia – Social and Behavioral Sciences* 53: 155–165.

Nielsen, J. C. O.; Oscarsson, J. 2004. Simulation of dynamic train–track interaction with state dependent track properties, *Journal Sound Vibration* 275: 515–532. http://dx.doi.org/10.1016/j.jsv.2003.06.033

Uzzal, R. U. A. 2012. *Analysis of a three dimensional railway vehicle–track system and development of a smart wheelset*: PhD thesis. Department of Mechanical and Industrial, Concordia University Montreal, Quebec, Canada. 261 p.

Wasiwitono, U.; Zheng, D.; Chiu, W. K. 2007. How useful is track acceleration for monitoring impact loads generated by wheel defects?, in *5th Australasian Congress on Applied Mechanics ACAM 2007*, 10–12 December 2007, Brisbane, Australia, 502–507.

Wu, T. X.; Thompson, D. J. 2001. *A hybrid model for wheel/track dynamic interaction and noise generation due to wheel flats.* ISVR Technical Memorandum 859, Institute of Sound and Vibration Research. 51 p.

Zhu, J. J.; Ahmed, A. K. W.; Rakheja, S. 2007. Adaptive contact model for simulation of wheel-rail impact load due to a wheel flat, in *13th National Conference on Mechanisms and Machines (NaCoMM07–046), IISc*, 12–13 December 2007, Bangalore, India, 157–164.

DINAMINĖS SISTEMOS „GELEŽINKELIŲ VAGONO RATAS – KELIAS“ SU RATO IŠČIUOŽA MATEMATINIS MODELIS IR MODELIAVIMO REZULTATAI

R. Žygienė, M. Bogdevičius, L. Dabulevičienė

Santrauka

Sukurtas sistemos „Geležinkelių vagono ratas – kelias“ su aširačio rato iščiuoža matematinis modelis. Sistema „Geležinkelių vagono ratas – kelias“ nagrinėjama vertikalioje plokštumoje. Sistemos „Geležinkelių vagono ratas – kelias“ matematiniame modelyje yra panaudoti tiesiniai ir netiesiniai tamprieji ir slopinimo diskretiniai elementai. Bėgio dinamika aprašoma baigtinių elementų metodu. Kontakte tarp bėgio ir aširačio rato su iščiuoža įvertinti bėgio ir aširačio rato nelygumai.

Atlikta geležinkelio vagono rato su iščiuoža, judančio greičiu $V = 60$ km/val., dinaminių procesų analizė.

Pateikti šios dinaminės sistemos matematinio modeliavimo rezultatai. Tyrimų rezultatai pavaizduoti grafiškai ir pateiktos tyrimų išvados.

Reikšminiai žodžiai: rato bėgio kontaktas, dinamika, pagreitis, penetracija, skaitinis metodas.